Materials Research. 2017; 20(5): 1322-1331
DOI: http://dx.doi.org/10.1590/1980-5373-MR-2016-0615

Photocatalytic Performance of Titanates with Formula $MTiO_3$ (M= Fe, Ni, and Co) Synthesized by Solvo-Combustion Method

María Elvira Zarazúa Morín[a]*, Leticia Torres-Martínez[a], Daniel Sanchez-Martínez[a],

Christian Gómez-Solís[a]

[a]Departamento de Ecomateriales y Energía, Facultad de Ingeniería Civil, Universidad Autónoma de Nuevo León - UANL, Ave. Universidad S/N, C.P. 64451, San Nicolás de los Garza Nuevo León, México

Received: August 23, 2016; Revised: June 13, 2017; Accepted: July 03, 2017

This work reports the synthesis of a variety of materials with an ilmenite-type structure $MTiO_3$ formula, where M= Fe, Co, and Ni, these materials were synthesized by the method of solvo-combustion, a simple and rapid method. These materials were characterized by X-ray Diffraction (XRD), scanning electron microscopy (SEM), FT-IR spectroscopy, thermogravimetric analysis (TGA/DTA), surface area determination by the BET method and analysis of particle size. The photocatalytic activity was measured in the degradation reactions of Rhodamine B (rhB) and tetracycline (TC). The results show that the crystallinity and surface area are factors that influence significantly on the photocatalytic activity of the synthesized titanates.

Keywords: *Non-aqueous solution, Characterization, Titanates, solvo-combustion, organic pollutants, photocatalysis*

1. Introduction

The materials based on ilmenite-structured titanates with formula $MTiO_3$ include metals such as nickel, cobalt, zinc, iron and copper among others. These compounds are universally known as inorganic functional materials with wide applications. These have a rhombohedral crystal structure of the R-3H space group with a hexagonal packing of the oxygen atoms occupying 2/3 of the octahedral positions, where M and Ti occupy alternating layers. The titanates of transition metals like Fe, Ni, Co-own diverse properties such as electricity, magnetism and semiconductivity[1-4]. These properties make titanates widely used in industry, for example, such as semiconductor rectifiers, electrodes of a solid oxide fuel cell, metal-air barrier, hydro-carbonate catalyzers, color mixtures for surface coating and gas sensing devices, among other applications[5-10].

Moreover, the application of titanates as photocatalysts is attracting considerable attention for the water and air purification. Pei-honget. al.[11] reported that the use of $NiTiO_3$ as a photocatalyst for degradation of humic acid in water, reached 95.3% after a 2.5 h reaction under irradiation of UV light. B.Gao and collaborators[12], found that commercial $FeTiO_3$ shows strong absorption in the visible region, so it could be used as a photocatalyst. F. Liu et al[13] report.that, the $FeTiO_3$ showed excellent results in the reduction of NO in presence of NH_3 at a conversion of 90%. Babu et al.[14] reported that it is possible to obtain photocatalytic activity by visible-light of $NiTiO_3$ thin films doped with nitrogen. Moghiminia et al. have tested $NiTiO_3$ and according to them, is an excellent photocatalyst and catalyst for several reactions, in this case, the activity was attributed to the synthesis method by sol-gel[15,16]. Another important factor is that these materials have a band gap energy (Eg) attractive that makes them active in the visible region as reported by Aguiet. al[17]. They published a study on charge transfer and optical properties of $MTiO_3$ (M =Mn, Fe, Co, and Ni), getting values of the band gap between 2.4-2.8 eV. Using the distance between the spectra edges of XAS and XES.

On the other hand, the typical ilmenites can be obtained by different routes of synthesis, but the most popular are the one based on the reaction of titania with other oxides or carbonates in solid state reactions at high temperatures (>1200 ºC). This method provides significant amounts of the required product with uniformed particle dimensions[8,18,19], on the other hand, the drawback of this method is its low surface area of the obtained solids; usually close at 1 m^2/g. They also have been synthesized by precursor polymers[5,11], mechanochemistry[9], sol-gel[20,21], and pechini[22]. Some of these methods require long reaction time and high-temperature calcination to obtained better properties. For this reason, the reaction conditions are one of the challenges today for the optimization and preparation of materials with unique properties.

Therefore, in this work we present the results of the synthesis and characterization of nickel titanate ($NiTiO_3$), cobalt titanate ($CoTiO_3$) and iron titanate ($FeTiO_3$) obtained by the solvo-combustion method. Also, the synthesized titanatesphotocatalytic activity was evaluated in the degradation

* e-mail: elzarazu@yahoo.com.mx

reactions of rhodamine B (rhB) and tetracycline (TC) under irradiation of visible light.

2. Experimental

2.1. Synthesis of titanates

The titanates were obtained by solvo- combustion method[23], using as precursors the Titanium (IV) n-butoxide (99%, Sigma-Aldrich), $Fe(NO)_3 \cdot 9H_2O$ (99.8% Fermont), cobalt (II) acetylacetonate (97%, Sigma-Aldrich) and nickel acetate (99% Sigma-Aldrich).

For $NiTiO_3$ synthesis, 6 x 10^{-3} mol of nickel acetate was placed in a flask and dissolved in 0.15 mol of acetylacetone with 0.26 mol of ethanol. Then 1.88 mL of titanium butoxide was added and perfectly mixed. The mixture was stirred and refluxed until 70 ºC. Then, 1 mL of nitric acid was added to the solution, and the flask was immediately placed onto a hot plate at 180 ºC to evaporate the solvents rapidly. During the evaporation, the sample spontaneously ignited, and in a few minutes, a black and spongy powder was obtained. The same procedure was used for the titanates of cobalt and iron. The obtained powders were calcined at different temperatures.

2.2. Characterization of the samples

The Thermal decomposition of the materials was investigated by thermogravimetric analysis (TGA) and differential thermal analysis (DTA) in SDTQ600 TA Instruments; the samples were heated with 10ºC/min from room temperature to 900 ºC, under the flow of 10mL/min in N_2. Structural characterization was carried out by X-ray powder diffraction using a Bruker D8 Advanced diffractometer with Cukα radiation (λ=1.5418Å) provided with a Vantec high-speed detector and Ni filters. X-ray diffraction data were collected in the range 2θ of 10-90º with a scan rate of 0.05º/second. The morphology of the samples was analyzed by scanning electron microscopy using a JEOL JSM 6490LV equipped with microanalysis dispersion X-ray (EDS) for its quantification.

UV-vis diffuse reflectance spectrums of the samples were measured using a UV-vis spectrophotometer (Perkin-Elmer Lambda 35) equipped with an integration sphere. The Eg was determined by the equation of energy Eg = hc/l.[24]. The Brunauer-Emmett-Teller (BET) surface area of the titanates was determined by N_2 adsorption-desorption measurements using a Quantachrome Nova 2000e Instruments. The isotherms of adsorption-desorption were evaluated at -196ºC after a sample pretreatment at 300ºC during 1h. The particle size and potential zeta was measurement using a Potesizer instrument. The sample was sonicated during 30 min, where the suspension was prepared by adding 50 mg of titanates to 100 mL of deionized water. The pH was adjusted using NaOH 1M and HCl 1M.

2.3. Photocatalytic experiments

The photocatalytic activity of the materials was determined by the degradation of rhodamine B and tetracycline in aqueous solution under irradiation of simulated sunlight. The experiments were carried out in a photochemical reactor system that has a Pyrex glass reactor (200 mL) equipped with an external water jacket to cool down the reaction mixture to room temperature. The system is illuminated with a Xe lamp of 35 W, 3200 lumens and 6000 K as a source of simulated sunlight, the lamp is settled in the center of the reactor. The fraction of radiation with a wavelength below 300 nm was filtered with a 5 M solution of sodium nitrite. For each experiment, 200 mL of rhodamine B standard solution (5 ppm) and tetracycline (20ppm) respectively were placed inside the glass reactor and mixed with 200 mg of the solid photocatalyst. The slurry was mixed with a magnetic stirrer at 500rpm, staying in darkness for 60min to reach the adsorption equilibrium. Then the Xe lamp was a turn on, and samples were taken at different time intervals to the progress of the reaction by UV-vis spectroscopy. These chemical analyses were carried out with a Perkin-Elmer Lambda 35 UV-vis spectrometer. Therefore, the fluorescence technique was used to detect of OH radicals formed on the surface of stannates using terephthalic acid; which reacts with OH radicals generating compounds with a strong fluorescent[25].

3. Results and Discussion

With the purpose to investigate the thermal behavior of the precursors used in the synthesis of titanates TGA and DTA measurements were performed, the respective curves are presented in Fig. 1(a-c). The Figure 1(a) corresponds to $FeTiO_3$ obtained under nitrogen flow, the first part of the TGA curve shows a weight loss below 300ºC that can be associated with the loss of occluded water in the starting material and to the combustion of organic material. Furthermore, DTA shows two exothermic peaks at 226 and 268ºC, which can be attributed to the combustion of organic material. The broad exothermic peak between 500 and 800ºC may be related to the crystallization of iron titanate ($FeTiO_3$)[6,22].

In Figure 1(b) shows the DTA/ TGA of the cobalt titanatewich present a weight loss around of 150ºC due to elimination of water and evaporation of organic matters and two exothermic peaks at 435. That those associated with the formation of Co_3O_4, and 505ºC were probably attributed of crystallization, in the range of 550-900ºC shows a slight weight loss that could be assigned to the oxygen removal during the formation of $CoTiO_3$ and Co_3O_4[9,26].

Figure 1(c) shows the thermal analysis the nickel titanate, this material present a weight loss at 200ºC, which corresponds to an endothermic peak due to the liberation of water and one-second weight loss between 390 and 638 ºC due to decomposition of organic material. These results

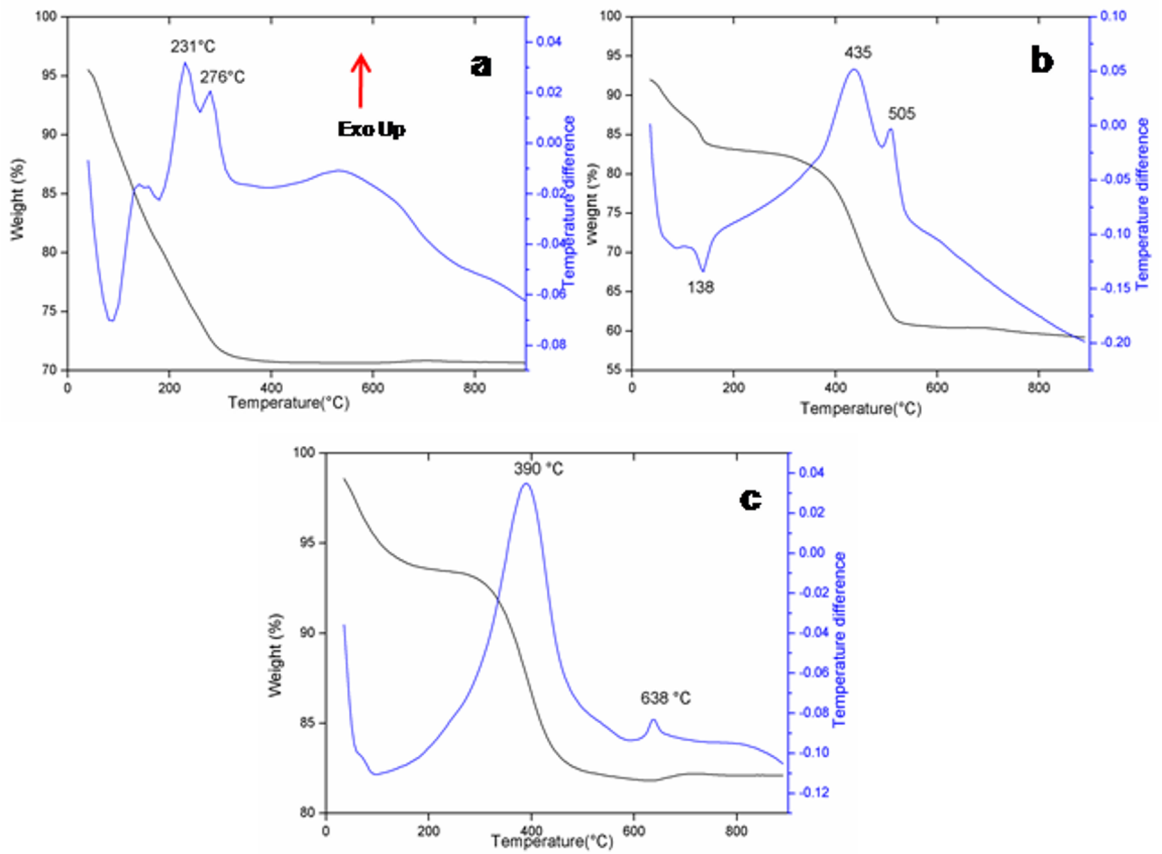

Figure 1. TG/DTA curves of (a) $FeTiO_3$ (b) $CoTiO_3$ and (c) $NiTiO_3$ at a heating rate of 10ºC/min from room temperature at 900 ºC, under the flow of 10mL/min in N_2.

are associated with an endothermic peak and at 638ºC, an exothermic peak that is related with the crystallization of the material. According to the results of XRD, the phase is obtained at 600ºC[5,11,27,28].

XRD patterns of the iron, cobalt and nickel titanate powders that were prepared by solvo-combustion method are shown in Figure 2. In the Figure 2(a) is shown the XRD patterns of $FeTiO_3$ synthesized and calcined at different temperatures under a nitrogen atmosphere. Where it can be seen that the sample at as prepared an amorphous structure material was obtained, treated at 600ºC for 5 hours indicates the formation of ilmenite with rhombohedral crystal structure according to the JCPDS 075-1208 file and traces of titanium oxide corresponding to the rutile phase JCPDS 021-1276. The three lines in Figure 2(a) shows that pure crystalline ilmenite ($FeTiO_3$) with major reflections at 23.97º, 33.04º, 35.67º, 40.90º, 49.32º, 53.76º, 57.09º, 62.36º and 64.20º is obtained after calcination at 700ºC for ten hours. These results confirm that pure ilmenite ($FeTiO_3$) has a rhombohedral crystal structure with the R-3H space group[6,13,22].

The Figure 2(b) shows the diffractogram of cobalt titanate obtained by solvo-combustion method as dried and calcined at 600 and 700ºC for 2h, observed its formation according to the database JCPDS 77-1373. The XRD pattern of the sample treated at 600ºC for 2 hours indicates the formation of the small reflections of ilmenite ($CoTiO_3$) with rhombohedral crystal structure according to the JCPDS 77-1373 file. Hovewer was detected low-intensity reflections corresponding to TiO_2 in the rutile phase (JCPDS 01-2176) and reflections associated with Co_3O_4 (JCPDS 04-31003)[9,19]. When the temperature was increased to 700ºC / 2h, the $CoTiO_3$ was obtained in its pure phase.

Figure 2 (c) shows the diffractograms of NiTiO3 powder thermal treatments for two hours in air atmosphere. In the first line is presented as prepared materials, the results revealed a low crystallinity of the NiO phase (JCPDS 89-3080), it was identified reflexions at 37º and 43º (2q). As annealing temperature was increased at 500 ºC, the reflexions associated to NiO increase slightly. When the temperature was at 600 ºC, it was observed more clearly the presence of the ilmenite ($NiTiO_3$) phase with a rhombohedric structure according to the database JCPDS 33-0960[8,9,27].

In the diffractograms of the three pure phases, where it can be seen that are isostructural and that the reflexions are shifted lightly, this result is natural for the variation of the radius of the cation Fe, Co, and Ni (see Figure 3). The results

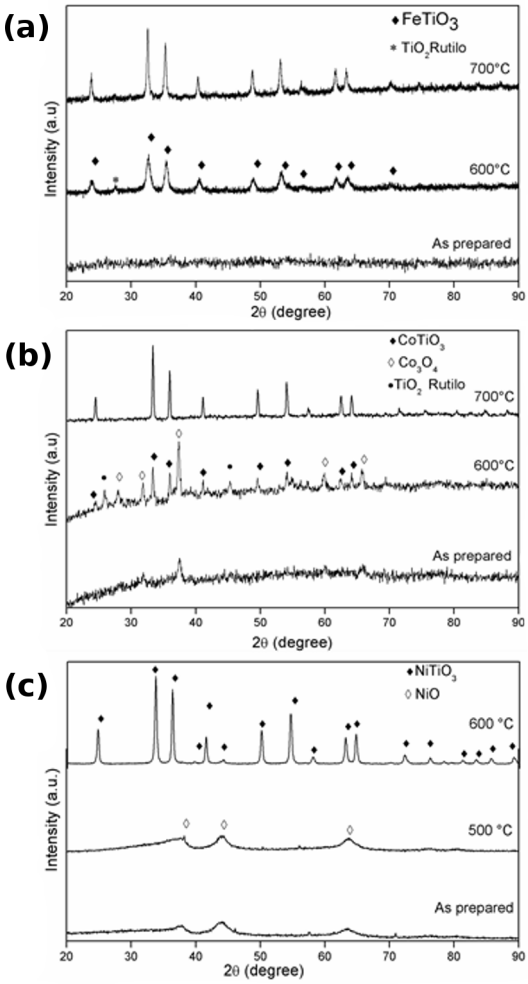

Figure 2. X-ray diffraction patterns of (a) $FeTiO_3$ (b) $CoTiO_3$ and (c) $NiTiO_3$ photocatalysts made by solvo-combustion synthesis after heat treatments at various temperatures for 2 h in air.

of scanning electron microscopy analysis of iron (FeTiO3), cobalt ($CoTiO_3$) and nickel ($NiTiO_3$) titanate synthesized by solvo-combustion are presented in the Figure 4. The micrographs obtained of the photocatalysts as prepared are presented in Figure 4 (a, c and e) these powders have similar morphology, particles of different sizes with large pores that can be seen in the precursor material. As the temperature was increased to 700ºC for $FeTiO_3$, $CoTiO_3$ and 600 ºC for $NiTiO_3$ (see Figure 4 b, d and f respectively), this image show the formation of foam morphology agglomerates with the presence of pores of different sizes. Olso it is observed, they nickel and cobalt titanates exhibit very similar pore sizes with values greater than 1µ, unlike iron titanate with larger pores, on de the other hand it is important mention this type of morphology which could be important factor for photocatalytic applications, favoring a greater diffusion of energy on the surface of the catalyst generating a greater amount of the electron-hole pair therefore greater production of free radicals.These morphology features are associated with the nature of the combustion reaction.

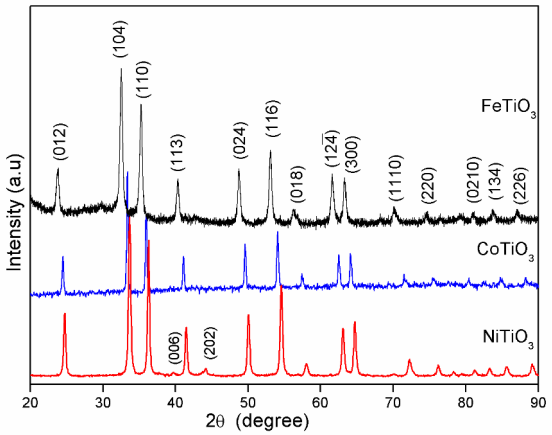

Figure 3. X-ray diffraction patterns of (a) $FeTiO_3$ (b) $CoTiO_3$ and (c) $NiTiO_3$ calcined at 700ºC /10 h, 700º C /2 h and 600 ºC/2h respectively.

The results of the elemental analysis (Figure 5) of these materials by EDS clearly indicate that the chemical composition corresponds to iron, cobalt, and nickel titanate. Figure 5(b) also shows the results of the chemical analysis of $CoTiO_3$ by atomic absorption spectroscopy, which indicates an atomic relationship between Co and Ti close to 1. Both chemical analyses confirm that the stoichiometry of the material corresponds to the ilmenite ($CoTiO_3$) and corroborate the results of X-ray diffraction. Moreover, the particle size distribution are showed in Figure 6. The $NiTiO_3$ shows the smaller particle size distribution between 15-80 nm. $CoTiO_3$ material presented the majority of the particle size distribution between 50 and 400 nm. Furthermore, the ilmenite $FeTiO_3$ showed a two different agglomerate distribution particle sized, one between 10 to 100 nm and the second between 100 to 300 nm. Likewise, the zeta potentials of titanates materials measured as a function of pH are showed in Figure 7. Where is clear to observed that the potential zeta become negative when the pH become more basic and the isoelectric point (IEPs) of the materials obtained by reading the intercept of the trend lines with the horizontal line of zero mV is 4.4, 5.4 and 5.7 for $FeTiO_3$, $CoTiO_3$ and $NiTiO_3$ respectively.

In the other hand, the specific surface area calculated by the BET method is shown in Table 1; The $CoTiO_3$ exhibited surface area low, and this valor indicates that the material morphology plays a significant role in determining textural properties as well as its crystallinity. It is well known it is a crucial element for use in photocatalysis. In this case, the $NiTiO_3$ has larger surface area.

3.1. Photocatalytic activity

The photocatalytic activity of titanates $MTiO_3$ (M= Fe, Ni, Co), was evaluated by analyzing the degradation of rhodamine B and tetracycline aqueous solution under Xe lamp irradiation. All the samples during the reactions were analyzed by UV-vis spectroscopy. Figure 8 show the

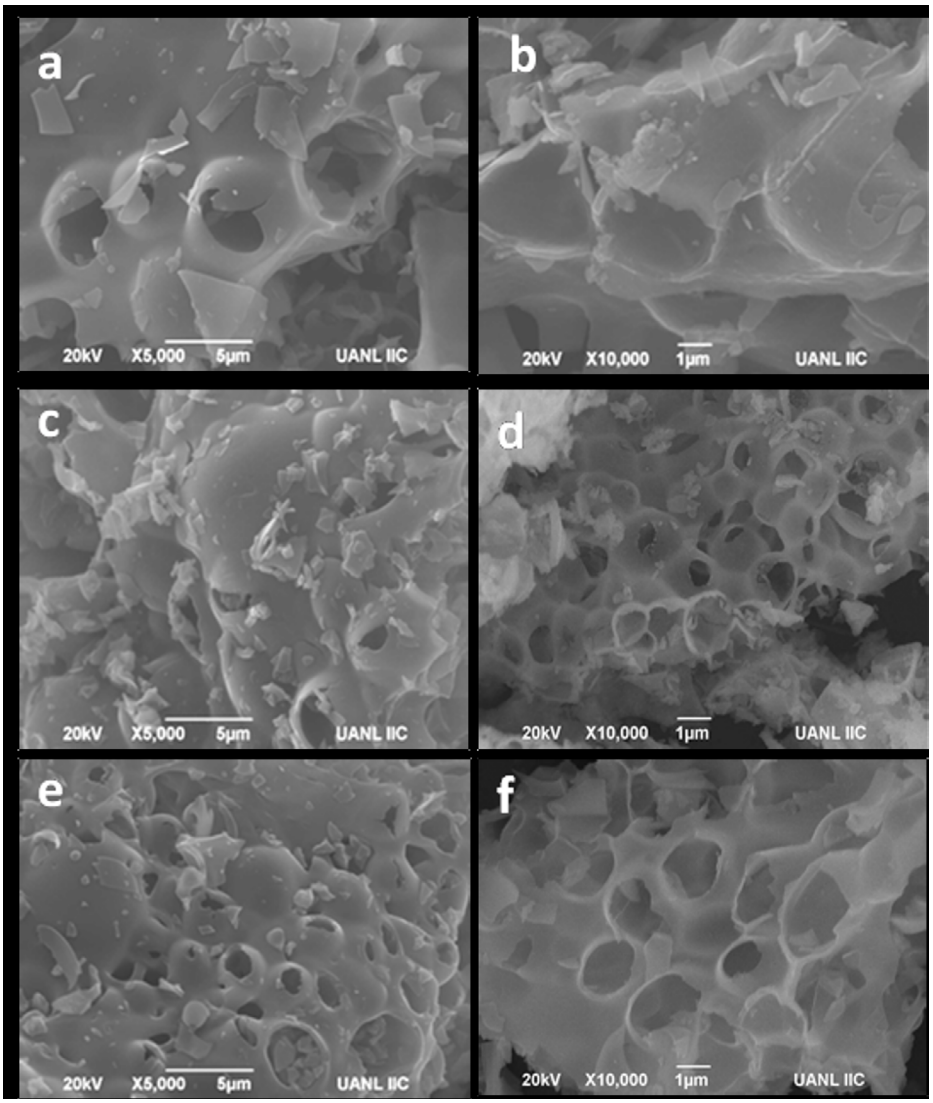

Figure 4. SEM microphotograph (a,b) $FeTiO_3$, (c,d) $CoTiO_3$ and (e,f) $NiTiO_3$ calcined at 700ºC / 10h , 700ºC/2h and 600º C/2h.

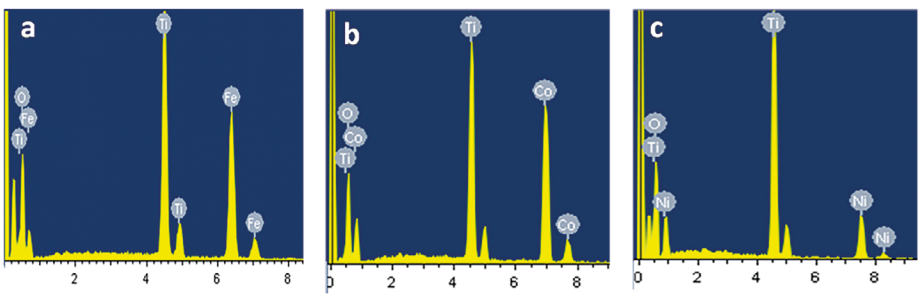

Elements	%Weight (EDS)	%Atomic (EDS)
Oxygen	32	60.39
Titanium	32	20.17
Iron	36	19.43

Elements	%Weight (EDS)	%Atomic (EDS)
Oxygen	31.40	60.30
Titanium	32.1	20.60
Cobalt	36	19.10

Elements	%Weight (EDS)	%Atomic (EDS)
Oxygen	31	60.03
Titanium	31	20.06
Iron	38	19.91

Figure 5. EDX and elemental chemical analysis of (a) $FeTiO_3$(b) $CoTiO_3$ and (c) $NiTiO_3$ obtained by solvo-combustion method and calcined at 700ºC /10 h, 700º C /2 h and 600 ºC/2h respectively.

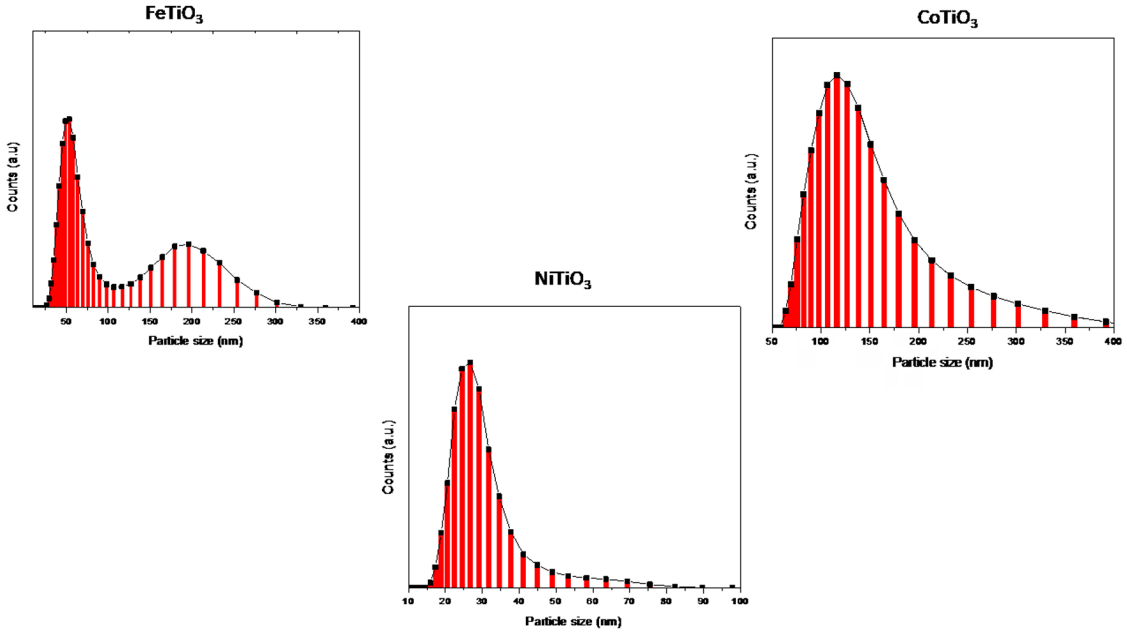

Figure 6. Particle size distribution histogram of the photoctalysts $FeTiO_3$, $CoTiO_3$, and $NiTiO_3$ sinthesized by solvo-combustion method.

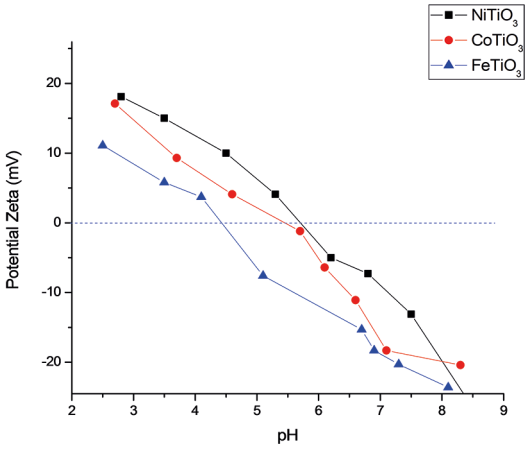

Figure 7. Zeta potentials of the titanates synthetized by the solvo-combuation method measured as a function of pH.

evolution of the concentration of rhB as a function of time during the experiment with different titanates.

The degradation of rhodamine B was calculated using the absorbance values of the band associated with the color (l =554nm). As seen in Figure 8(a) which clearly indicates that rhodamine B is not degraded by a simple photochemical effect of light with wavelength larger than 554 nm. Also shows that pure ilmenite ($FeTiO_3$) does not have any photocatalytic activity, When the rhodamine B solution was irradiated with visible light in the presence the $CoTiO_3$, is observed a slight degradation in the model molecule, being around 30%. In the case of $NiTiO_3$, the degradation of rhodamine B is faster than with $FeTiO_3$ and $CoTiO_3$, achieving 48% degradation of the dye in five hours, as shown Figure 8.

The results obtained of UV-vis spectra after different illumination times with the nickel titanate are shown in Figure 8(b). In the picture, it can be seen that the main absorbance of rhodamine B at 554 nm gradually shifted to a shorter wavelength. At 120 min the wavelength of maximum absorbance was changed to 551nm, finishing at 538 nm hypsochromic effect, according to what reported by Xiukai Lee et al., this effect causes the de-ethylated product of the rhodamine B molecule. In this case, the displacement in the maximum absorbance band indicates that ethylation was carried out gradually, resulting in the formation of N, N, N-tri-ethylated rhodamine, intermediates formed do not degrade quickly, so the percentage degradation of rhodamine B was only 48%.

These materials were also evaluated in the photocatalytic degradation of tetracycline molecule at 20 ppm irradiated by the lamp Xe of 35 W during 300 min. In Figure 9 is shown the UV-Vis spectrum obtained. During photolysis, tetracycline concentration decreases around 15% as seen in

Table 1. Energy band gap and BET surface area of $FeTiO_3$, $CoTiO_3$ and $NiTiO_3$ photocatalysts.

Photoatalyst	Temperature	Eg (eV)	Bet (m^2/g)
$FeTiO_3$	700 ºC/ 10h	2.7	10
$CoTiO_3$	700 ºC/ 2h	2.6	15
$NiTiO_3$	600 ºC/ 2h	2.8	26

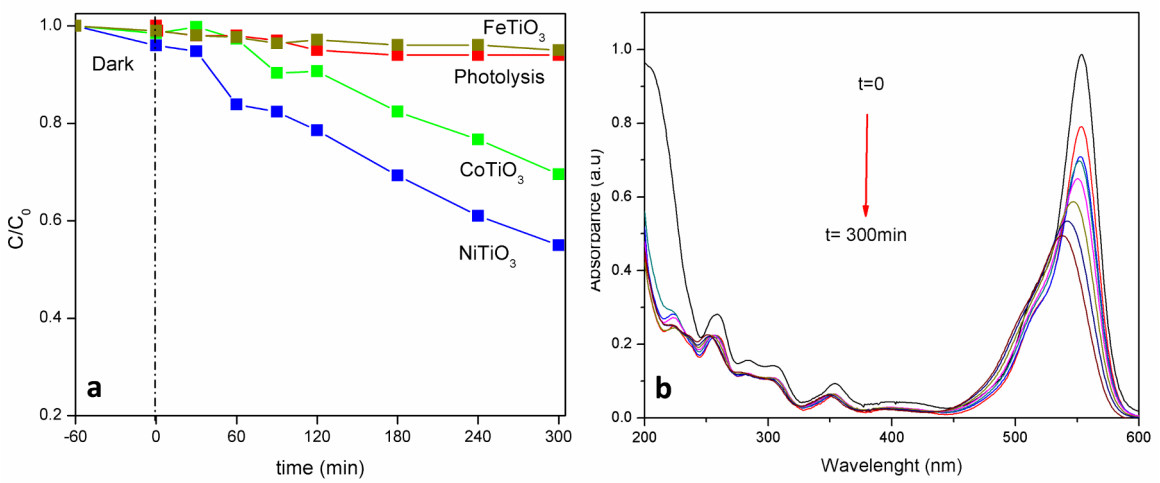

Figure 8. Photocatalytic degradation of an aqueous solution of Rhodamine B with the photocatalyst. $FeTiO_3$, $CoTiO_3$, and $NiTiO_3$ monitored by UV-vis spectroscopy and relative concentration of rhodamine B as a function of time with $NiTiO_3$.

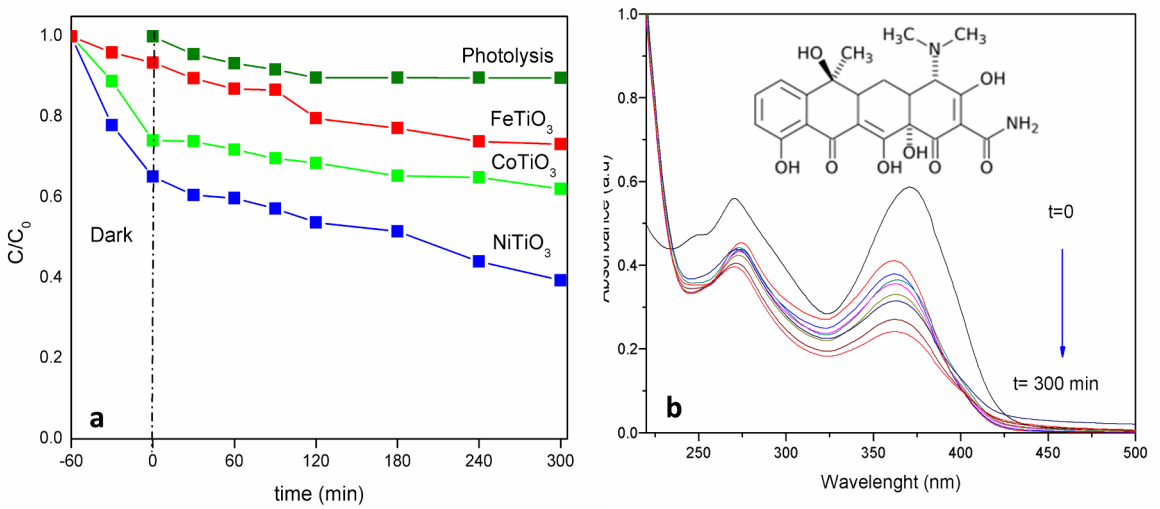

Figure 9. Photocatalytic degradation of an aqueous solution of Tetracycline with the phases synthesized by solvo-combustion method, the samples were analyzed by UV-vis spectroscopy and relative concentration of the drug as a function of time during the Photocatalytic degradation with $NiTiO_3$.

Figure 9(a), in the darkness, the $NiTiO_3$ presents a 35% TC absorption, while for $CoTiO_3$ and $FeTiO_3$ was 26% and 7% respectively. On the other hand, this can be due to the $NiTiO_3$ greater surface area as compared to other photocatalysts. Thus, $NiTiO_3$ could provide more adsorption sites for TC[29].

Figure 9(b) shows the UV-Vis spectra of the photocatalytic degradation of an aqueous solution of tetracycline with the titanates of nickel, cobalt and iron illuminated with visible light. This figure clearly indicates that the absorbance of the band located at 368 nm decreases with the reaction time indicating rupture of phenolic groups to aromatic rings B, also shows that the absorbance of the bands located at 270 nm decrease with reaction time, we can attribute this to the production of acylamino and hydroxyl groups. These results suggest that they are a by-product, which is more recalcitrant and therefore difficult to eliminate at 100%[30,31].

In addition it was determined the mineralization degree of the titanates synthetized after the photocatalytic degradation of rhodamine B and TC. For these tests the $NiTiO_3$ and $CoTiO_3$ with the highest photocatalytic activity was used as the photocatalyst, After 5 h the reaction, the mineralization aproximately. of 24% for $NiTiO_3$ and 18% for $CoTiO_3$ by rhodamine B. with respect to the TC only the $NiTiO_3$ was evaluated obtaining around 15% of mineralization.

As shown in Figure 10, we can see the gradual increment in fluorescence at about 430 nm for the three titanates. Furthermore, the $NiTiO_3$ material showed the highest fluorescence intensity in comparison with $CoTiO_3$ and $FeTiO_3$. This result suggests that a larger amount of ·OH radicals are generated for $NiTiO_3$, which corroborates the capacity to degradation of Rhodamine B and tetracycline. Where this results is concordant with R. A Palominos et al. where

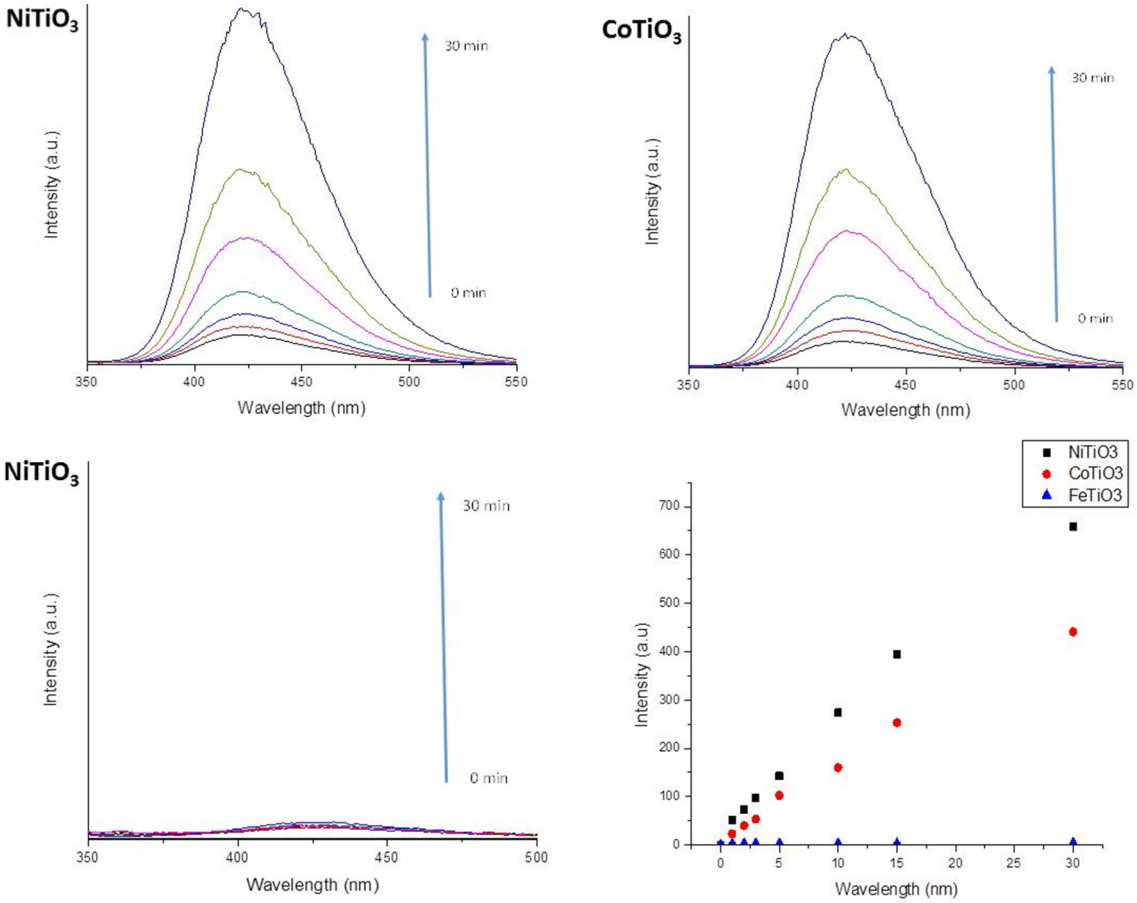

Figure 10. Fluorescence spectra of $NiTiO_3$, $CoTiO_3$ and $FeTiO_3$ obtained by solvo-combustion method and calcined at 600 ºC/ 2h , 700 ºC/2h and 700 ºC/10h respectively.

indicate the hydroxyl radical plays a significant role in the oxidation of tetracycline[32]. However, the activity probably was affected by the amount of holes and HO· radicals generated, may be that the reaction follows the mechanism reported by J. Niu et al. where indicate that the HO·, O_2^- and the h_{vb}^+ are either not involved in the decomposition of tetracycline, or not be the main reactive species during the photocatalysis[33].

On the other hand, having a solution near to a pH 7, the particle size of $NiTiO_3$ present the smaller size, which favors the migration of electron-hole pair, therefore, it can be observed that increasing the particle size and agglomerate formation, the photocatalytic activity decreases. The results of zeta potential can be seen that even pH close to 7 of the titanate particles will be kept to a negative value favoring the dispersion in the suspension. Thus, according to these results the titanates can be applied to photocatalyst for tetracycline and Rhodamine B degradation. Trying to increased photocatalytic activity, using any co-catalyst to help generate species that act directly in the degradation of pollutants. So, although titanates exhibit lower activity with respect to other materials[32,33,34], they can be a good alternative as support for other catalysts improving significantly the activity.

4. Conclusion

Pure iron, cobalt, and nickel titanates were obtained directly and quickly by solvo-combustion method. The materials synthesized were evaluated in the photocatalytic degradation of two model molecules, these being a dye (Rhodamine B) and a drug (tetracycline) and irradiated under simulated sunlight and for this purpose a Xe lamp was employed. The photocatalyst that showed greater degradation of these molecules was nickel titanate with 48% for rhodamine B and 61% for tetracycline, so we can conclude that factors as surface area, bandwidth morphology, and the high ability to produce OH radicals are factors that proved decisive to propose these materials as ideal candidates for application in photoinduced processes.

5. Acknowledgments

Authors would like to thank the financial support for this research to CONACYT through projects: CB-2013-220802, CB-2014-237049, INFRA-2015-252753, SEP-PROFOCIE-2014-19-MSU0011T-18, SEP-INTEGRACIÓN DE REDES

TEMÁTICAS 2015-CA-244 103.5/15/14156, UANL-PAICYT 2015 and FIC-UANL-PAIFIC 2015,

6. References

1. Nguyen-Phan TD, Huy CN, Kim CK, Shin EW. Facile microwave-assisted synthesis and controllable architecture of three-dimensional nickel titanate. *CrystEngComm*. 2015;17(24):4562-4574.

2. Fujii T, Oohashi H, Tochio T, Ito Y, Vlaicu AM, Fukushim S. Speculations on anomalous chemical states of Ti ions in $FeTiO_3$ observed by high-resolution X-ray Kβ emission spectra. *Journal of Electron Spectroscopy and Related Phenomena*. 2011;184(1-2):10-15.

3. Liu XC, Hong R, Tian C. Tolerance factor and the stability discussion of ABO_3-type ilmenite. *Journal of Materials Science: Materials in Electronics*. 2009;20:323.

4. Liferovich RP, Mitchell RH. Rhombohedral ilmenite group nickel titanates with Zn, Mg, and Mn: synthesis and crystal structures. *Physics and Chemistry of Minerals*. 2005;32(5-6):442-449.

5. Sadjadi MS, Zare K, Khanahmadzadeh S, Enhessari M. Structural characterization of $NiTiO_3$ nanopowders prepared by stearic acid gel method. *Material Letters*. 2008;62(21-22):3679-3681.

6. Tang X, Hu K. The formation of ilmenite $FeTiO_3$ powders by a novel liquid mix and H_2/H_2O reduction process. *Journal of Materials Science*. 2006;41(23):8025-8028.

7. Klemme S, Hermes W, Eul M, Wijbrans CH, Rohrbach A, Pöttgen R. New thermodynamic data for $CoTiO_3$, $NiTiO_3$ and $CoCO_3$ based on low-temperature calorimetric measurements. *Chemistry Central Journal*. 2011;5:54. DOI: 10.1186/1752-153X-5-54

8. Chuang SH, Hsieh ML, Wu SC, Lin HC, Chao TS, Hou TH. Fabrication and Characterization of High-k Dielectric Nickel Titanate Thin Films Using a Modified Sol-Gel Method. *Journal of the American Ceramic Society*. 2011;94(1):250-254.

9. Lin YJ, Chang YH, Yang WD, Tsai BS. Synthesis and characterization of ilmenite $NiTiO_3$ and $CoTiO_3$ prepared by a modified Pechini method. *Journal of Non-Crystalline Solids*. 2006;352(8):789-794.

10. Enhessari M, Moqhadam SN, Razi MK, Ghezelbashi S, Tootkani MH. Synthesis and characterizations of $CoTiO_3$-clay nanocomposites by sol-gel method. *International Journal of Nano Dimension*. 2010;1(2):125-132.

11. Yuan PH, Fan CM, Ding GY, Wang YF, Zhang XC. Preparation and photocatalytic properties of ilmenite $NiTiO_3$ powders for degradation of humic acid in water. *International Journal of Minerals, Metallurgy, and Materials*. 2012;19(4):772-776.

12. Gao B, Kim YJ, Chakraborty AK, Lee WI. Efficient decomposition of organic compounds with $FeTiO_3/TiO_2$ heterojunction under visible light irradiation. *Applied Catalysis B: Environmental*. 2008;83(3-4):202-207.

13. Liu F, He H, Zhang C. Novel iron titanate catalyst for the selective catalytic reduction of NO with NH_3 in the medium temperature range. *Chemical Communications (Camb)*. 2008;(17):2043-2045.

14. Bellam JB, Ruiz-Preciado MA, Edely M, Szade J, Jouanneauxa A, Kassiba AH. Visible-light photocatalytic activity of nitrogendoped $NiTiO_3$ thin films prepared by a cosputtering process. *RSC Advances*. 2015;5(14):10551-10559.

15. Moghiminia S, Farsi H, Raissi H. Comparative optical and electrochemical studies of nanostructured $NiTiO_3$ and $NiTiO_3$-TiO_2 prepared by a low temperature modified Sol-Gel route. *Electrochimica Acta*. 2014;132:512-523.

16. Traistaru GA, Covaliu CI, Oprea O, Matei V, Matei D, Cursaru D, et al. $MTiO_3$ (M=Cu,Ni) as Catalysts in Toluene Oxidation. *Revista de Chimie (Bucharest)*. 2011;62(8)773-776.

17. Agui A, Mizumaki M. Intermetallic charge transfer and band gap of $MTiO_3$ (M = Mn, Fe, Co, and Ni) studied by O 1s-edge X-ray emission spectroscopy. *Journal of Electron Spectroscopy and Related Phenomena*. 2011;184(8-10):463-467.

18. Ohara S, Sato K, Tan Z. Novel mechanochemical synthesis of fine $FeTiO_3$ nanoparticles by a high-speed ball-milling process. *Journal of Alloys and Compounds*. 2010;504(1):L17-L19.

19. Chuang SH, Gao RH, Wang DY, Liu HP, Chen LM, Chiang MY. Synthesis and Characterization of Ilmenite-Type Cobalt Titanate Powder. *Journal of the Chinese Chemical Society*. 2010;57(4B):932-937.

20. Traistaru GA, Covaliu CI, Matei V, Cusaru D, Jitaru I. Synthesis and characterization of $NiTiO_3$ and $NiFe_2O_4$ as catalysts for toluene oxidation. *Digest Journal of Nanomaterials and Biostructures*. 2011;6(3):1257-1263.

21. Jacob KT, Raj S, Reddy SNS. Activities in the $FeTiO_3$-$NiTiO_3$ Solid Solution from Alloy-Oxide Equilibria at 1273 K. *Journal of Phase Equilibria and Diffusion*. 2009;30(2):127-135.

22. Mona J, Kale SN, Gaikwad AB, Murugan AV, Ravi V. Chemical methods to synthesize $FeTiO_3$ powders. *Materials Letters*. 2006;60(11):1425-1427.

23. Ruiz-Gómez MA, Gómez-Solís C, Zarazúa-Morín ME, Torres-Martínez LM, Juárez-Ramírez I, Sánchez-Martínez D, et al. Innovative solvo-combustion route for the rapid synthesis of MoO_3 and Sm_2O_3 materials. *Ceramics International*. 2014;40(1 PtB):1893-1899.

24. Ibañez JG, Solorza O, Gómez-del-Campo E. Preparation of Semiconducting Materials in the Laboratory: Production of CdS thin films and estimation of their band gap energy. *Journal of Chemical Education*. 1991;68(10):872.

25. Ishibashi KI, Fujishima A, Watanabe T, Hashimoto K. Detection of active oxidative species in TiO_2 photocatalysis using the fluorescence technique. *Electrochemistry Communications*. 2000;2(3):207-210.

26. Gabal MA, Hameed SA, Obaid AY. $CoTiO_3$ via cobalt oxalate-TiO_2 precursor. Synthesis and characterization. *Materials Characterization*. 2009;71:87-94.

27. Lopes KP, Cavalcante LS, Simões AZ, Varela JA, Longo E, Leite ER. $NiTiO_3$ powders obtained by polymeric precursor method: Synthesis and characterization. *Journal of Alloys and Compounds*. 2009;468(1-2):327-332.

28. Li X, Ye J. Photocatalytic Degradation of Rhodamine B over $Pb_3Nb_4O_{13}$/Fumed SiO_2 Composite under Visible Light Irradiation. *Journal of Physical Chemistry C*. 2007;111(35):13109-13116.

29. Chu X, Shan G, Chang C, Fu Y, Yue L, Zhu L. Effective degradation of tetracycline by mesoporous Bi_2WO_6 under visible light irradiation *Frontiers of Environmental Science & Engineering*. 2016;10(2):211-218.

30. Safari GH, Hoseini M, Seyedsalehi M, Kamani H, Jaafari J, Mahvi AH. Photocatalytic degradation of tetracycline using nanosized titanium dioxide in aqueous solution. *International Journal of Environmental Science and Technology*. 2015;12(2):603-616.

31. Zhu XD, Wang YJ, Sun RJ, Zhou DM. Photocatalytic degradation of tetracycline in aqueous solution by nanosized TiO_2. *Chemosphere*. 2013;92(8):925-932.

32. Palominos RA, Mondaca MA, Giraldo A, Peñuela G, Perez-Moya M, Mansilla HD. Photocatalytic oxidation of the antibiotic tetracycline on the TiO_2 and ZnO suspensions. *Catalysis Today*. 2009;144(1-2):100-105.

33. Niu J, Ding S, Zhang L, Zhao J, Feng C. Visible-light-mediated Sr-Bi_2O_3 photocatalysis of tetracycline: Kintetics, mechanisms and toxicity assessment. *Chemosphere*. 2013;93(1):1-8.

34. Reyes C, Fernández J, Freer J, Mondaca MA, Zaror C, Malato S, et al. Degradation and inactivation of tetracycline by TiO_2 photocatalysis. *Journal of Photochemistry and Photobiology A: Chemistry*. 2006;184(1-2):141-146.